# A D-Band Packaged Antenna on Low Temperature Co-Fired Ceramics for Wire-Bond Connection with an Indium Phosphide Power Meter

Bing Zhang, Li Wei and Herbert Zirath
Microwave Electronics Laboratory, Department of Microtechnology and Nanoscience MC2, Chalmers University of Technology, SE-41296, Gothenburg, Sweden
bing.zhang@chalmers.se

***Abstract*-A D-band packaged grid array antenna (GAA) on Ferro A6M low temperature co-fired ceramic (LTCC, $\varepsilon_r$ = 5.74, tan$\delta$ = 0.0023 @ 145 GHz) is presented. It is designed for wire-bond connection with an indium phosphide (InP) power meter as a demonstration of a D-band packaged radio. Dimensions of the GAA (*x*, *y*, *z*) = (12, 12, 0.5) mm$^3$. Simulated by Ansoft HFSS, the antenna's impedance bandwidth is 139 - 149.3 GHz, maximum gain of 20.9 dBi @ 147.8 GHz with 3-dB gain bandwidth 139.5 – 150.8 GHz, vertical beams of 10$^o$ beamwidth in the broadside are detected 139 – 151 GHz on both E- and H-planes. The 25 um diameter co-planar bonding wires that bridge the InP chip and LTCC antenna substrate over a 250 um separation are studied, showing acceptable insertion loss and limited bandwidth.**

## I. Introduction

The D-band radiometer is attractive for real-time imaging, in which the system's angular resolution is directly related with the radiation beamwidth of the antenna [1]. Silicon lens are widely adopted for this application because of the focused beams over a wide spectrum [2]. However, the relatively high fabrication cost of the silicon lens prevents its wide-spread industrial application which requires a cost-effective mass production capability. Moreover the protruding contour of a silicon lens can result in a bulky package that also contradicts the need for compact front-ends.

We investigate the antenna for D-band real-time imaging applications from the perspective of electromagnetics instead of the optical view. For the small wavelength of millimeter-wave (mmWave) spectrum, a single chip radio becomes possible in which most of the antennas fall into categories of antenna-on-chip (AoC) and antenna-in-package (AiP) [3]. In this paper, grid array antenna (GAA) is adopted on Ferro A6M low temperature co-fired ceramic (LTCC) as a D-band AiP prototype [4-7]. Simulated by Ansoft HFSS, the antenna shows comparable performance with the silicon lens [1], [2]. A cavity on the back of the GAA is designed to host an indium phosphide (InP) D-band power meter [8]. The co-planar boding wires bridging the InP power meter and the GAA are studied, showing acceptable insertion loss and narrow bandwidth.

## II. Design of the D-Band GAA

The GAA has dimensions of 12 mm × 12 mm × 0.5 mm in Fig. 1. It consists of four LTCC (in green) and five metallic layers (in brown). All the metallic layers are made of 0.01 mm thick gold (conductivity = 2.5 × 10$^8$ s/m). The radiating array (rad) is composed of 16 subarrays, each including 8 loops, with separation of 0.05 mm between the adjacent subarrays. The lengths of the short and long sides of each loop are 0.51 mm and 1.02 mm respectively. The widths of the loop short and long sides are governed by impedance, transmission and radiation properties [9]. The width of the short side of each loop is made equal to that of the long side which is 0.13 mm. The LTCC substrate layer for the radiating array (sub$_1$) is 0.2 mm thick. The metallic ground plane (gnd$_1$) is for the radiating elements and the stripline feeding network (sfn). In the LTCC process, it is difficult to achieve smooth finishing surface with lumped resistors that are sandwiched between two substrates. To overcome the problem, the ideal Wilkinson power splitters are replaced by T-junctions in sfn which eliminate the necessity of the lumped resistor to dissipate the odd mode. The ceramic substrates (sub$_2$ and sub$_3$) for the sfn have an equal thickness of 0.1 mm. The stripline feeding network has one input port and sixteen output ports. The sixteen output ports are connected to the sixteen subarrays respectively by vias of length 0.3 mm through sixteen circular openings on the gnd$_1$. The fencing vias of length 0.2 mm are located around each feeding via to connect the first and second ground planes. The fencing vias are designed for smooth transition between the sfn and rad. The sfn supports a transverse electromagnetic (TEM) mode whose equal phase front is perpendicular to gnd$_1$ and gnd$_1$, however equal phase front of the TEM mode on the feeding vias is parallel with gnd$_1$ and gnd$_2$. As expected, there will be diffraction, reflection as well as radiation when the input signal of the GAA is propagating from the sfn to the rad. Fences of more vias can ensure smoother field transition between the vertical and horizontal TEM modes, stronger suppression of the parallel-plate mode, as well as maintain an equal potential between ground planes gnd$_1$ and gnd$_2$. The 0.1 mm bottom ceramic layer (sub$_4$) provides the substrate for the ground-signal-ground (GSG) testing pad (tp) or the power, signal and ground traces to be wire-bonded with InP power meter. A cavity of dimensions (*x*, *y*, *z*) = (0.35, 2.5, 1) mm$^3$ is realized on sub$_4$ to host the InP power meter.

Simulated by Ansoft HFSS, the GAA shows impedance bandwidth 139 - 149.3 GHz in Fig. 1. In Fig. 2, the maximum gain of 20.9 dBi appears at 147.8 GHz with 3-dB gain bandwidth 139.5 – 150.8 GHz. Radiation patterns in Fig. 3 show vertical beams on both E- and H-planes from 139 – 151 GHz. The beamwidths are 8$^o$ @ 139 GHz with -10 dB side lobe level (SLL), 10$^o$ @ 145 GHz with -16.2 SLL and 10$^o$ @ 151 GHz with -20 dB SLL. Considering the high gain and broad impedance bandwidth of the GAA, it features a capable candidate for D-band imaging applications.

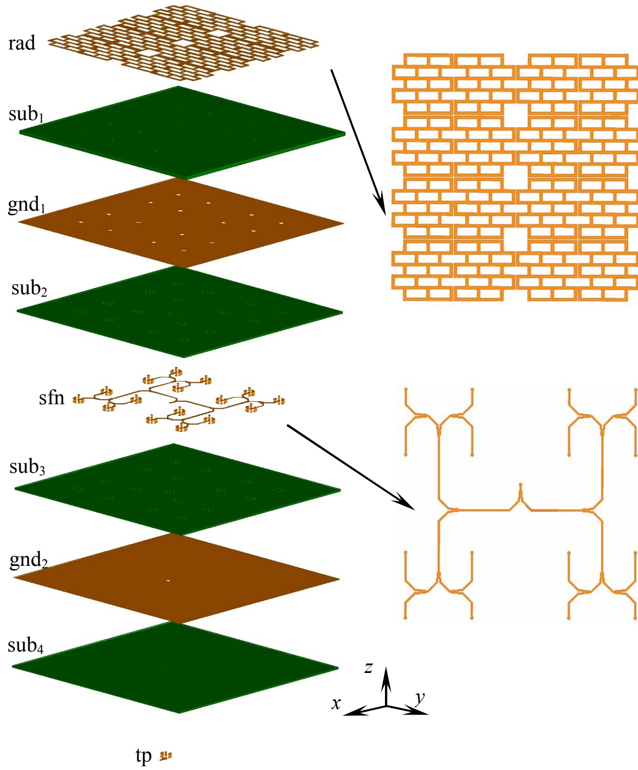


Fig. 1. Exploded view of the D-band GAA.

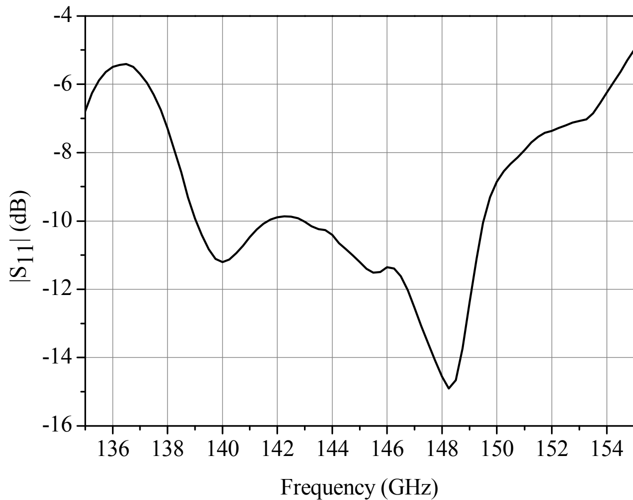


Fig. 2. Simulated $|S_{11}|$ of the D-band GAA.

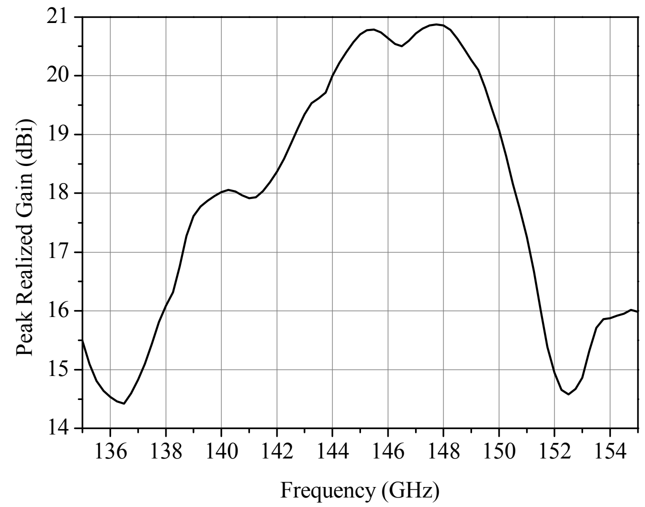


Fig. 3. Simulated peak realized gain of the D-band GAA.

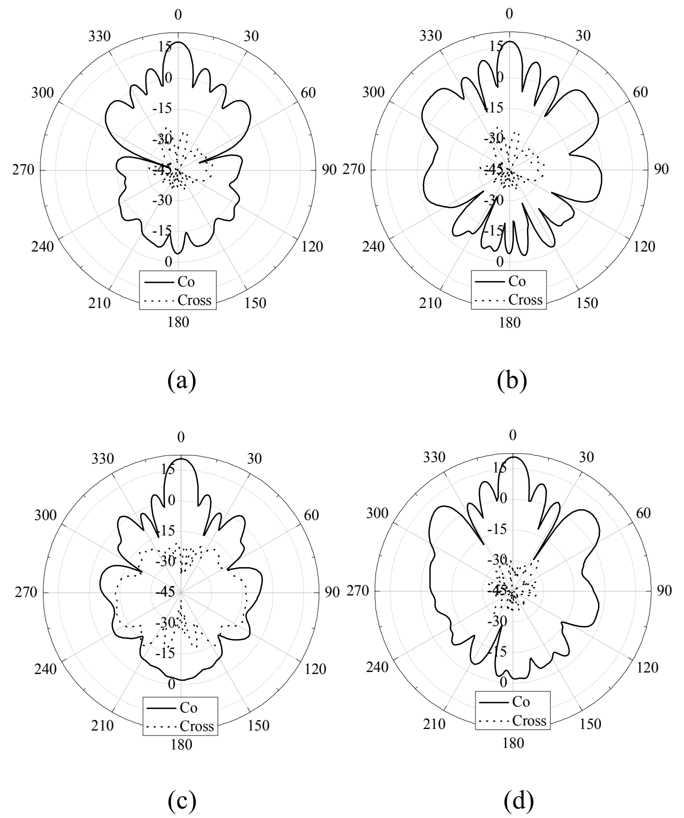

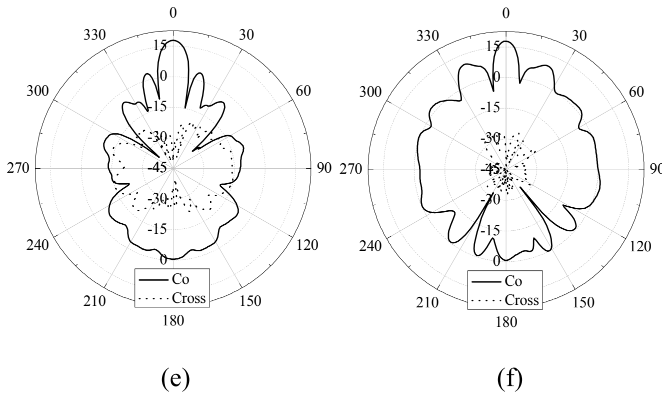


Fig. 4. Simulated radiation patterns of the D-band GAA: (a) 139 GHz E-plane, (b) 139 GHz H-plane, (c) 145 GHz E-plane, (d) 145 GHz H-plane, (e) 151 GHz E-plane and (f) 151 GHz H-plane.

## III. Study of the Co-Planar Bonding Wires

In this work, for the easy implementation and robustness against chip thermal expansion (or contraction), Au co-planar bonding wires of 25 um diameter are adopted to interconnect an InP power meter with the GAA in Fig. 1. They bridge over a separation of 250 um with dual-wire connections between the GSG pad on the benzocyclobutene (BCB, $\varepsilon_r = 2.7$) layer of 5 um thickness over the 100 um InP substrate and the other GSG pad on the Ferro A6M LTCC substrate of 100 um thickness as shown in Fig. 5. Port 2 is located at the end of the BCB substrate while Port 1 is located at the end of the LTCC substrate, on which matching stubs are designed for smoother transition.

At low frequencies, bonding wires are modeled as multi-stage low-pass filters with fixed cut-off frequency. The influential parasitic inductance is usually compensated by properly designed series capacitor [10]. As frequency increases, the length of bonding wire reaches significant fractions of wavelength and exhibits transmission line properties. As a result, the characteristic impedance and effective dielectric constant become dominant factors instead of the parasitic inductance. Former research focused on the specific condition of bonding wires over a uniform substrate [11]. In this paper, co-planar bonding wires overpass two different substrates will bring about drastic discontinuity of the characteristic impedance, which results in relatively high insertion loss and limited bandwidth. Simulated by Ansoft HFSS, it is shown in Fig. 6 that after de-embedding, the minimum insertion loss is 3.2 dB @ 146 GHz which is comparable with [12], the 3-dB pass band is 141-150 GHz. Since the GAA is going to be used as a receiving antenna, though the 3.2 dB insertion loss is acceptable for power consideration it can double the noise level and decrease the sensitivity of the following InP power meter. The input impedance at Port 1 ($|S_{11}| < -10$ dB) is 144.5 – 147.5 GHz, which is not broad enough for imaging applications. Future work will be involved in the optimization of the bonding wires for lower insertion loss and broader bandwidth.

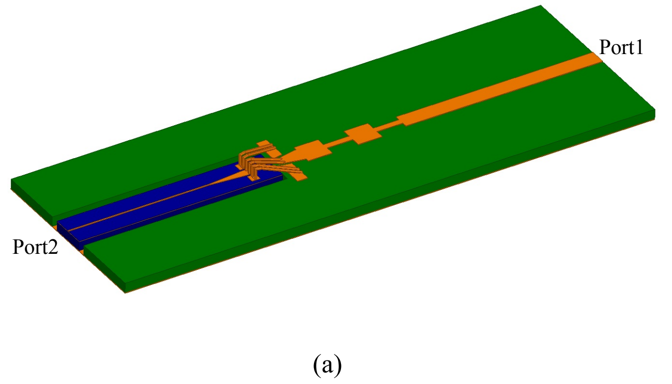


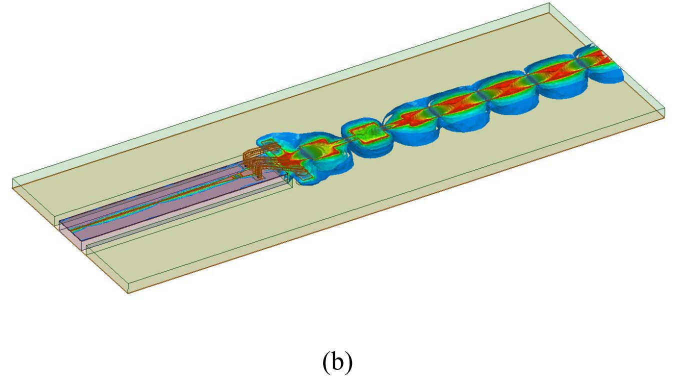


Fig. 5. Wire-bond connection between the InP power meter and the LTCC GAA: (a) HFSS model and (b) E-field distribution at 146 GHz.

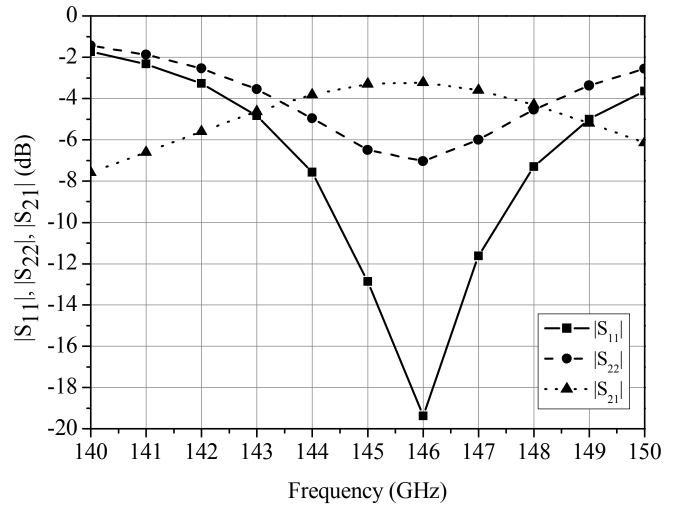


Fig. 6. Simulated frequency response of the wire-bond connection between the InP power meter and LTCC GAA.

## IV. Conclusions

In this paper, a GAA is designed on Ferro A6M LTCC substrate to be wire-bonded with a D-band InP power meter. Simulated by Ansoft HFSS, it shows comparable performance with silicon lens in terms of gain and beamwidth, while

having advantages as conformal profile and the elimination of extra package. However, the design of bonding wires that connect the LTCC GAA and InP power meter shows large insertion loss as well as limited bandwidth for the discontinuity of the characteristic impedance over the BCB band the LTCC substrates. Further effort will be taken into the optimization of the bonding wires for low insertion loss and broad bandwidth.

## ACKNOWLEDGMENT

The author would like to thank Vessen Vassilev and Vedran Furtula for the discussion on the InP power meter, as well as Bertil Hansson and Per-Åke Nilsson for the assistance in chip dicing. The author would also like to thank Zhongxia He, Niklas Wadefalk and Marcus Gavell for the discussion on bonding wires, and Mattias Ferndahl for probe testing of the antenna.

## REFERENCES

[1] Y. Yan, Y. B. Karandikar, S. E. Gunnarsson, B. M. Motlagh, S. Cherednichenko, I. Kallfass, A. Leuther, and H. Zirath, "Monolithically integrated 200-GH double-slot antenna and resistive mixers in a GaAs-mHEMT MMIC process," *IEEE Trans. Microw. Theory Tech.*, vol. 59, no. 10, pp. 2494-2503, Oct. 2011.

[2] D. F. Filipovic, S. S. Gearhart and G. M. Rebeiz, "Double-slot antennas on extended hemispherical and elliptical silicon dielectric lens," *IEEE Trans. Microw. Theory Tech.*, vol. 41, no. 10, pp. 1738-1749, Oct. 1993.

[3] Y. P. Zhang and D. Liu, "Antenna-on-chip and antenna-in-package solutions to highly integrated millimeter-wave devices for wireless communications," *IEEE Trans. Antennas Propag.*, vol. 57, no. 10, pp. 2830-2841, Oct. 2009.

[4] J. D. Kraus, "A backward angle-fire array antenna," *IEEE Trans. Antennas Propag.*, vol. 12, pp. 48-50, Jan. 1964.

[5] H. Nakano, T. Kawano, H. Mimaki, and J. Yamauchi, "A fast MoM calculation technique using sinusoidal basis and testing functions for a wire on a dielectric substrate and its application to meander loop and grid array antennas," *IEEE Trans. Antennas Propag.*, vol. 53, no. 10, pp. 3300-3307, Oct. 2005.

[6] B. Zhang, D. Titz, F. Ferrero, C. Luxey, and Y. P. Zhang, "Integration of quadruple linearly-polarized microstrip grid array antennas for 60-GHz antenna-in-package applications," *IEEE Trans. Comp. Packag. Manuf. Technol.*, in press.

[7] S. Beer, C. Rusch, B. Göttel, H. Gulan, and T. Zwick, "D-band grid-array antenna integrated in the lid of a surface-mountable chip-pakcage," *EuCAP2013*, Gothenburg, Sweden, Apr. 8-12, 2013, pp. 1273-1277.

[8] V. Vassilev, H. Zirath, V. Furtula, Y. Karandikar and K. Eriksson, "140-220 GHz imaging front-end based on 250 nm InP/InGaAs/InP DHBT process," in *Proc. Defence Security+Sensing Technical Program SPIE 2013*, Baltimore, Maryland, Apr. 29 – May 3, 2013.

[9] B. Zhang and Y. P. Zhang, "Analysis and synthesis of millimeter-wave microstrip grid array antennas," *IEEE Antennas Propag. Mag.*, vol. 53, no.6, pp. 42-55, Dec. 2011.

[10] Y. P. Zhang, M. Sun, K. M. Chua, L. L. Wai, and D. Liu, "Antenna-in-package design for wirebond interconnection to highly integrated 60-GHz radios," *IEEE Trans. Antennas. Propag.*, vol. 57, no. 10, pp. 2842-2852, Oct. 2009.

[11] K. W. Goossen, "On the design of coplanar bond wires as transmission lines," *IEEE Microw. Guid. Wave Lett.*, vol. 9, no. 12, pp. 511-513, Dec. 1999.

[12] T. Krems, W. Haydl, H. Massler, and J. Rudiger, "Millimeter-wave performance of chip interconnections using wire bonding and flip chip," in *IEEE MTT-S Int. Microwave Symp. Dig.,* vol. 1, San Francisco, CA, Jun. 1996, pp. 247- 250.